Anisotropic Responses of Mechanical and Thermal Processed Cast Al-Si-Mg-Cu Alloy

S.O. ADEOSUN,[1,4] E.I. AKPAN,[2,5] S.A. BALOGUN,[3,6] and O.K. ONOYEMI[1]

1.—Department of Metallurgical and Materials Engineering, University of Lagos, Lagos, Nigeria. 2.—Department of Materials and Production Engineering, Ambrose Alli University, Ekpoma, Nigeria. 3.—Department of Mechanical and Biomedical Engineering, Bells University of Technology, Ota, Nigeria. 4.—e-mail: samsonoluropo@yahoo.com. 5.—e-mail: emma_eia@yahoo.com. 6.—e-mail: sanmbo2003@yahoo.co.uk

The effects of ambient directional rolling and heat treatments on ultimate tensile strength (UTS), hardness (HD), percent elongation (PE), and impact energy (IE) on Al-Si-Mg-Cu alloy casting with reference to inclination to rolling direction are discussed in this article. The results show that rolled and quenched (CQ) sample possess superior UTS and HD to as-cast and those of rolled and aged samples (CA). Improved IE resistance with ductility is shown by both CQ and CA samples. However, these mechanical properties are enhanced as changes in the test sample direction moved away from rolling direction for all heat-treated samples. The CQ samples displayed highest tensile strength (108 MPa) and PE (19.8%) in the 90° direction.

INTRODUCTION

Al-Si-Mg-Cu cast alloys are important light metals used widely in aerospace, automotive, and household because of their excellent mechanical properties and castability.[1,2] They are useful as supercharger covers, fuel-pomp bodies, air-compressor pistons, liquid-cooled aircraft engine crankcases, motor mounts, cylinder heads, heat exchangers, air conditioners, transmissions housings, wheels, fenders, loads, and floor and suspension components due to room and elevated temperature strengths.[3–6] The main alloying elements (Si, Cu, and Mg) are known to partly dissolve in the primary alpha-Al matrix during melting and solidification leading to the formation of important intermetallic phases making the alloy susceptible to heat treatment for improved mechanical properties.[6]

The most common heat treatment for these alloys is T6, comprising solution treatment, quenching, and artificial aging. The study of Mohamed and Samuel[7] shows that Al-Si-Cu-Mg alloys possess high age-hardening response. The equilibrium phase diagrams of Al-Mg-Si-Cu alloys presented by several authors show metastable phases indicating the possibility of precipitation strengthening.[8–13] The study of Chaudhury and Apelian[14] shows that solution heat treatment of the alloy leads to increased ultimate tensile strength (UTS) and ductility, whereas aging increases yield strength (YS) at the expense of ductility. Gauthier et al.[15] investigated solution heat treatment of 319 alloys over a temperature range of 480°C to 540°C, for solution times of up to 24 h. They reported a good combination of tensile strength and ductility when solution heat treated at 515°C for 8–16 h, followed by quenching in warm water at 60°C. Sokolowski et al.[16] shows that a two-step solution treatment at 495°C/2 h followed by 515°C/4 h produce an optimum combination of strength and ductility for 319 alloy compared with the traditional single-step solution treatment of 495°C/8 h. Ouellet and Samuel[17] used a solution temperature of 500°C to achieve improvement in mechanical properties in Al-Si-Cu-Mg. Wang et al.[18] also reported increase in all tested mechanical properties for a similar alloy with a solution temperature of 520°C.

These studies show that in precipitation hardening, cold deformation before quenching, and aging offer an improved rate of strengthening. This is attributed to the high rate of precipitation-induced super saturated solid solution of θ'', θ', and θ precipitates. A study on Al-Cu-Mg alloy shows that cold deformation prior to aging enhances nucleation of precipitates resulting in relative increase in hardness.[19] However, the influence of ambient

deformation and heat treatments on Al-Si-Mg-Cu alloy processed with respect to the direction of deformation has not been considered. This article examines the anisotropic responses of this alloy to deformation and subsequent heat treatment.

EXPERIMENTAL METHODOLOGY

The composition of Al-Si-Mg-Cu alloy used for this study is given in Table I. Fifteen kilograms of this alloy was charged into a crucible, placed in a pit furnace, and heated until molten at 670°C. The molten alloy was poured into prepared sand molds and allowed to solidify. The casts were divided into three groups: control samples (AC); cold-rolled, solution-treated, and quenched sample (CQ); and

cold-rolled, solution-treated, and aged (CA). CQ and CA samples were initially homogenized in a Carbolite furnace at 510°C for 8 h, air cooled, and cold rolled from 350 mm × 150 mm × 15 mm (at 26°C surface temperature) to 270 mm × 131 mm × 13.5 mm in four passes (at 34.4°C surface temperature).

Standard tensile test pieces were machined in accordance to ASTM E8 standard from AC, CQ, and CA samples at 0°, 15°, 30°, 45°, 60°, 75°, and 90° to the rolling direction. Similarly, standard impact and hardness tests pieces were machined from these samples (see Fig. 1). CQ and AC test pieces were subjected to solution heat treatment at 510°C for 8 h. Subsequently, CQ test pieces were quenched in water while CA test pieces were quenched and

Table I. Chemical Composition of Al-Si-Mg-Cu Alloy

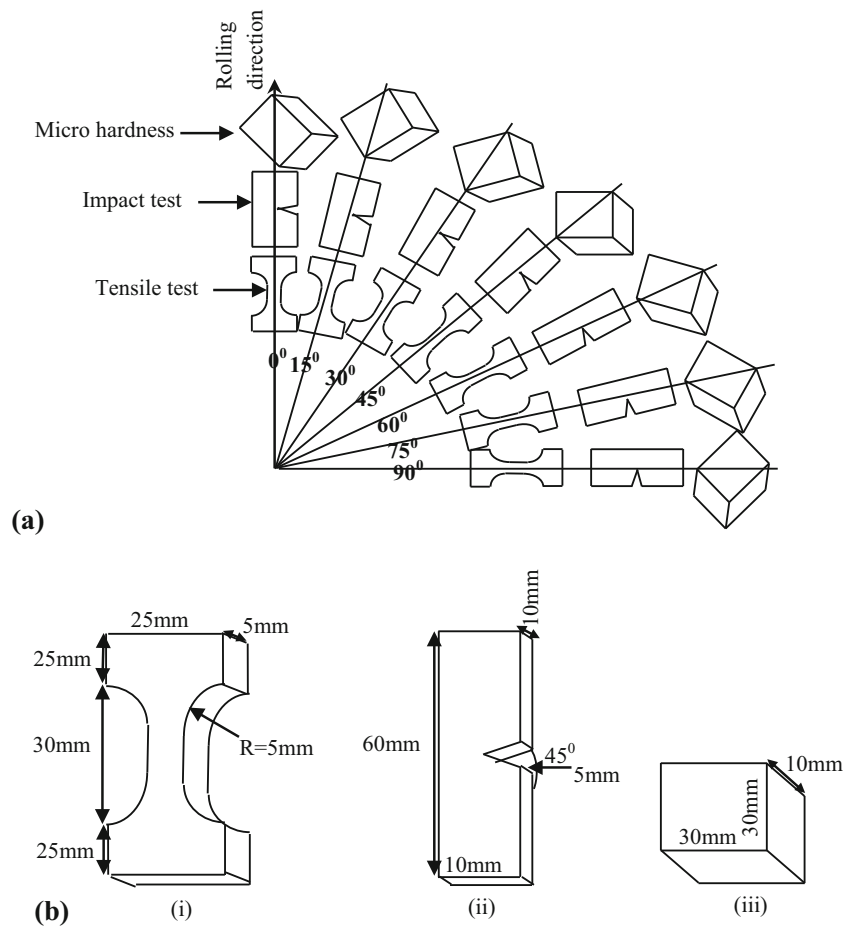| Element	Al	Na	Pb	Mg	Si	Fe	Mn	Ti	Zn	Ni	Cu
Percent composition	97.1	0.02	0.05	0.36	1.18	0.85	0.02	0.01	0.12	0.01	0.28

Fig. 1. (a) Test pieces cut at different angles to the rolling direction. (b) Standard test samples: (i) tensile, (ii) impact, and (iii) hardness.
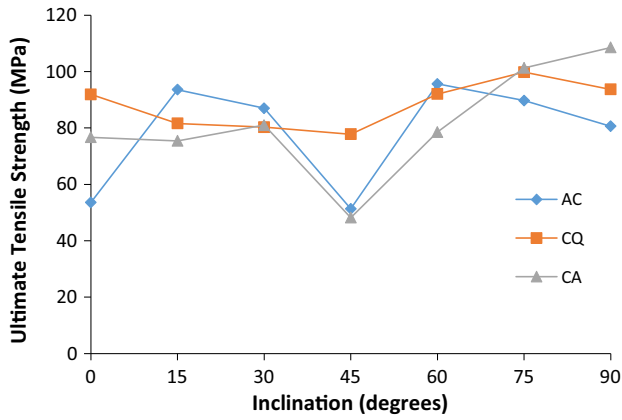
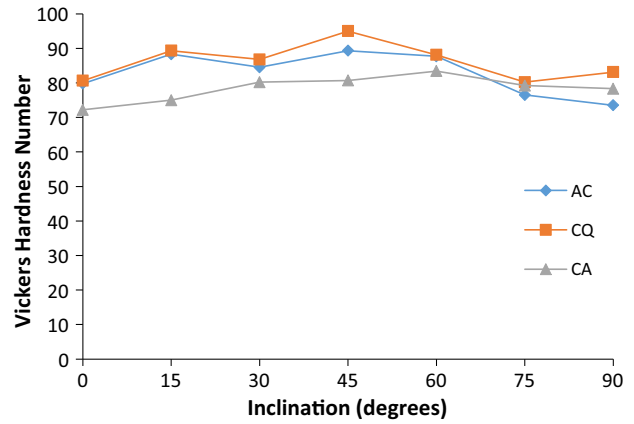Fig. 2. Ultimate tensile strength with inclination.
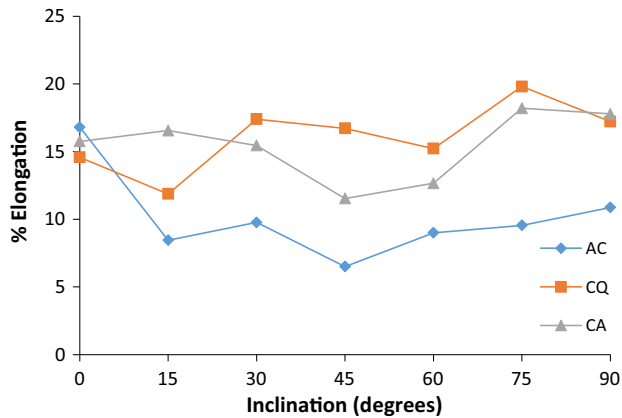

Fig. 4. Vicker's hardness with inclination.

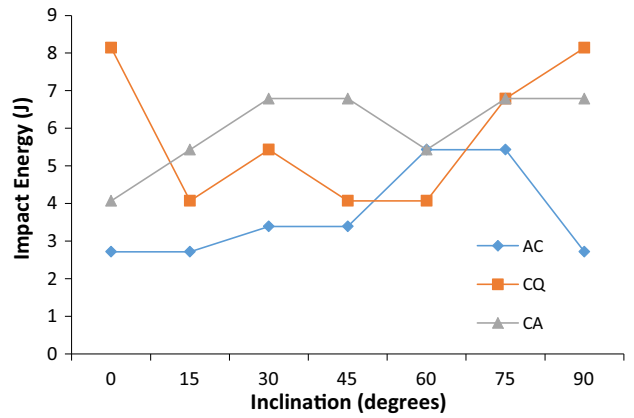Fig. 3. Percentage elongation with inclination.

Fig. 5. Impact energy with inclination.

artificially aged at 190°C for 8 h and air cooled to room temperature.

Twenty-one samples were tested for tensile, hardness, and impact for the three groups. A Vickers microhardness tester model "Deco" 2005 with a test load of 100 g and a dwell time of 10 s was used for the sample hardness determination. An Avery impact testing machine (Charpy Tester, model 6703, serial number E67424/4) with a striking velocity of 298.1 J/s was used to determine the impact energy absorption capacity of samples.

A digital metallurgical microscope was used to examine the microstructure of processed samples. Standard microstructural test pieces from AC, CQ, and CA were ground using emery paper with grit of 220 to 600 microns in succession. The ground surfaces of the test pieces are polished using a mixture of Al_2O_3 and diamond paste before etching in a solution containing 5 g of sodium hydroxide (NaOH) dissolved in 100 mL of water for 20 s and dried. The etched samples were examined using a digital metallurgical microscope at 100× magnification and the photomicrographs are shown in Fig. 6a–i.

RESULTS

Figures 2, 3, 4 and 5 show the results of mechanical properties of the alloys. Figure 2 shows the variation of UTS with increase in angle of inclination with respect to the rolling direction. In the rolling direction CQ show the highest tensile strength of 93 MPa followed by CA (78 MPa) and AC (54 MPa). An increase in inclination angle led to an initial decrease in the tensile strength of the CQ sample reaching a minimum at 45° direction after which it increases steadily with a further increase in the angle of inclination to a maximum of 100 MPa at 75°. CA and AC samples show fluctuating strength patterns with minimum UTS of 50 and 54 MPa, respectively, at 45°. The CA samples show maximum tensile strength (108.53 MPa) at 90°, whereas the AC samples show maximum tensile strength at 15°.

The variation of ductility of processed samples with the angle of inclination is shown in Fig. 3. The AC samples experience a gradual decrease in ductility with an increase in inclination angle to a minimum (6.5%) at 45° but tend to increase with a

Fig. 6. Micrographs of (a) as-cast at 0; (b) cold rolled at 0; (c) homogenized, cold rolled, and quenched at 0 (d); homogenized, cold rolled, and precipitation hardened at 0 (e); as-cast at 45; (f) homogenized, cold rolled, and quenched at 45; (g) cold rolled and precipitation hardened at 45 (h); as-cast at 90; (i) homogenized, cold rolled, and quenched at 90; and (j) cold rolled and precipitation hardened at 90.

further increase in inclination angle to a maximum (10%) at 90°. All AC samples are found to possess inferior ductility to that in the direction of rolling. The CQ sample demonstrates improved ductility with increase in inclination angle reaching a maximum (17.5%) at 75°. The CQ and CA samples have peak elongations of 20% and 18%, respectively in the 75° direction.

Figure 4 presents the measured Vicker's hardness number for the processed samples. The hardness of all samples increases with inclination until a maximum is attained at 60° for the CA sample and 45° in the AC and CQ samples. A further increase in inclination angle leads to a decline in hardness for all the samples. The CQ and AC samples exhibit superior hardness to the CA sample at all inclination angles except 75° and 90°.

The variation of impact energy of the samples with angle of inclination is shown in Fig. 5. The impact energy absorption of the AC sample increases with the inclination angle to a peak (5.5 J) at 60° before it declines with a further increase in the inclination angle. The CA sample shows a higher impact energy response over AC at 45° (6.9 J) but a decrease at 60° (5.5 J). The impact energy increase afterwards with further increase in inclination angle to a maximum of 6.9 J at 75° and 90° directions. The CQ sample shows superior

toughness (8.2 J) in rolling and 90° directions. It is clearly shown that the CQ sample possesses the best toughness.

DISCUSSION

It is generally observed that the microstructures (Fig. 6a–g) of the alloy consist of precipitates of Mg_2Si and intermetallic phases like $AlCu_2$ and AlSiFeMg in the α-aluminum matrix. In Fig. 6a, Mg_2Si crystals dominate in the α-aluminum matrix, with fine crystals of $AlCu_2$ and AlSiFeMg evenly distributed in the matrix. Precipitation hardening strengthens the alloy due to the $AlCu_2$, Mg_2Si, and AlSiFeMg precipitates formed. The precipitates severely strained the α-aluminum matrix resulting in an increased hardness and UTS of the alloy. The presence of iron ($>0.5\%$) has a tendency to reduce the strength and hardness of the alloy in heat-treated conditions; however, the formation of α-FeSi occasioned by the silicon content (1.18%) prevented the decline in these properties.[20] Figure 6b–d consists of the as-cast, quenched, and aged samples morphologies in the direction of rolling. AC and CQ samples (Fig. 6b, c) have similar structures containing fine crystals of Mg_2Si and AlSiFeMg with approximately equal volume fractions. The crystals of Mg_2Si appear in the grain boundaries in the matrix while $AlCu_2$ and AlCuMgFe crystals are fairly distributed in the matrix. Some crystals of AlSiFeMg and $AlCu_2$ phases are found alternating with the α-aluminum crystals. This may be the reason for increased hardness and impact energy over the aged samples (see Figs. 4, 5). When aged, the Mg_2Si crystals increased in volume fraction, whereas other intermetallics such as $AlCu_2$ and AlSiFeMg earlier formed are reabsorbed into the solution (see Fig. 6d). It has been noted by Syahid et al.[21] that the presence of $AlCu_2$ and AlSiFeMg leads to an increase in the hardness property of the Al-Si-Cu-Mg alloy, supporting the earlier result that quenched and as-cast samples possessed superior hardness to the aged sample because they contain a higher volume fraction of fine $AlCu_2$ and AlSiFeMg precipitates.

Figure 6e (samples tested at 45° inclination) shows predominately crystals of α-aluminum with few Mg_2Si crystals at the grain boundaries. The AlCuMgFe crystals are seen in alternative layers with α-aluminum crystals and that of $AlCu_2$. However, the crystals of α-aluminum are more uniformly distributed than that in Fig. 6e (see Fig. 6f). AlCuMgFe crystals occur at the grain boundaries in this sample. In Fig. 6g, there is a decrease in volume fractions of $AlCu_2$ and AlCuMgFe phases when compared with Fig. 6e and f, resulting in a decrease in tensile elongation and hardness. Mg_2Si precipitates are found at the grain boundaries of the aged samples. These precipitates are fine and evenly dispersed in the matrix. The presence of incoherent Mg_2Si precipitates may be responsible for the

increase in impact energy over that of the as-cast and quenched samples (see Fig. 5).

Figure 6h–j shows the microstructures of alloys tested in the 90° orientation. There is strong precipitation of Mg_2Si crystals in Fig. 6h with a reduction in volume fractions of other intermetallics in α-aluminum matrix. In Fig. 6i, there is a significant reduction in the volume fractions of Mg_2Si, $AlCu_2$, and AlCuMgFe crystals in the matrix as these are held in solid solution of α-aluminum. Mg_2Si crystals, though few, are at the grain boundaries and are well distributed within matrix. The morphology of the sample in Fig. 6j is similar to that in Fig. 6i with a slight increase in the volume fraction of Mg_2Si in its matrix.

CONCLUSION

The quenched and aged samples have higher strengths and impact energy at 90° to the rolling direction due to morphology of the structures. There is a slight increase in the volume fraction of Mg_2Si in the matrix, which is largely responsible for the increase. The rolled and quenched samples at 75° and 90° to the rolling direction have higher strengths when compared with other samples. An appreciable increase in strength is also observed with the as-cast sample in the 15° direction. The quenched and aged samples are characterized with better ductility, as it increases from 18% to 20%. It is also observed that all the samples have high hardness values. However, the quenched sample is relatively higher in comparison with other samples.

REFERENCES

1. P.K. Rohatgi, D. Nath, S.S. Singh, and B.N. Keshavaram, *J. Mater. Sci.* 29, 5975 (1994).
2. C. Jeong, *Mater. Trans.* 54, 588 (2013).
3. L.A. Dobrzanski, W. Borek, and R. Maniara, *J. Achiev. Mater. Manuf. Eng.* 18, 211 (2006).
4. Z. Li, A.M. Samuel, F.H. Samuel, C. Ravindran, H.W. Doty, and S. Valtierra, *Mater. Sci. Eng. A* 367, 111 (2004).
5. Z. Li, A.M. Samuel, C. Rayindran, S. Valtierra, and H.W. Doty, *Mater. Sci. Eng.* 367, 111 (2004).
6. G. Mrówka-Nowotnik and J. Sieniawski, *Arch. Mater. Sci. Eng.* 47, 85 (2011).
7. M.A. Mohamed and F.H. Samuel, *Heat Treatment—Conventional and Novel Applications*, ed. F. Czerwinski (Rijeka, Croatia: Intech, 2012), pp. 55–72.
8. S.D. Dumolt, D.E. Laughlin, and J.C. Williams, *Scripta Metall.* 18, 1347 (1984).
9. D.J. Chakrabarti, B.K. Cheong, and D.E. Laughlin, *Automotive Alloys*, ed. S.K. Das (Warrendale, PA: TMS, 1998), p. 27.
10. W.F. Miao and D.E. Laughlin, *Scripta Mater.* 40, 873 (1999).
11. W.F. Miao and D.E. Laughlin, *Metall. Mater. Trans. A* 31A, 361 (2000).
12. W.F. Miao and D.E. Laughlin, *J. Mater. Sci. Lett.* 19, 201 (2000).
13. D.J. Chakrabarti, Y. Peng, and D.E. Laughlin (Paper presented at the 8th International Conference of Al Alloys, Cambridge, U.K., 2–5 July 2002).
14. S.K. Chaudhury and D. Apelian, *Metall. Mater. Trans. A* 37A, 2295 (2006).
15. J. Gauthier, P. Louchez, and F.H. Samuel, *Cast Metals* 8, 91 (1995).

16. J.H. Sokolowski, M.B. Djurdjevic, C.A. Kierkus, and D.O. Northwood, *J. Mater. Process. Technol.* 109, 174 (2001).
17. P. Ouellet and F.H. Samuel, *J. Mater. Sci.* 34, 4671 (1999).
18. P.S. Wang, S.L. Lee, and J.C. Lin, *J. Mater. Res.* 15, 2027 (2000).
19. N. Unlu, B.M. Gable, G.J. Shiflet, and E.A. Starke, *Metall. Mater. Trans.* 34, 2757 (2003).
20. V. Raghavan, *J. Phase Equilib. Diffus.* 28, 213 (2007).
21. M. Syahid, B.T. Sofyan, S.G. Basuki, and B. Adam, *Adv. Mater. Res.* 789, 324 (2013).